Conductivity enhancement in single-walled carbon nanotube bundles doped with K and Br

R. S. Lee*, H. J. Kim*, J. E. Fischer*, A. Thess† & R. E. Smalley†

** Department of Materials Science and Engineering and Laboratory for Research on the Structure of Matter, University of Pennsylvania, Philadelphia, Pennsylvania 19104-6272, USA*

† Center for Nanoscale Science and Technology, Rice Quantum Institute and Departments of Chemistry and Physics, Rice University, Houston, Texas 77251, USA

Single-walled carbon nanotubes (SWNTs), prepared by metal-catalysed laser ablation of graphite, form close-packed bundles or 'ropes'[1]. These rope crystallites exhibit metallic behaviour above 50 K (ref. 2), and individual tubes behave as molecular wires, exhibiting quantum effects at low temperatures[3,4]. They offer an all-carbon host lattice that, by analogy with graphite[5] and solid C_{60} (ref. 6), might form intercalation compounds with interesting electronic properties, such as enhanced electrical conductivity and superconductivity. Multi-walled nanotube materials have been doped with alkali metals[7] and $FeCl_3$ (ref. 8). Here we report the doping of bulk samples of SWNTs by vapour-phase reactions with bromine and potassium—a prototypical electron acceptor and donor respectively. Doping decreases the resistivity at 300 K by up to a factor of 30, and enlarges the region where the temperature coefficient of resistance is positive (the signature of metallic behaviour). These results suggest that doped SWNTs represent a new family of synthetic metals.

All experiments were performed on bulk (3×8 mm) unoriented samples, or 'mats', using four-point pressure contacts. We estimate that at least 70 vol.% of this material consists of achiral single-walled nanotubes (refs 1, 9, 10) which are predicted to be intrinsically metallic[11]. The correspondence between rope resistivity ρ and mat resistance is complicated by several factors. First, we can only access some average of tensor components (we expect $\rho_{\parallel} \ll \rho_{\perp}$ by analogy to graphite for which $\rho_a \ll \rho_c$, where the subscripts refer to current flow parallel and perpendicular to the tube axis, or parallel to the graphite *a* and *c* axes respectively). Second, we overestimate ρ if rope–rope contacts are more resistive than the ropes themselves. We expect this factor to be relatively minor owing to the extreme aspect ratio of the rope crystallites and the fact that the highly conducting direction coincides with the longer dimension; the number of rope–rope contacts between voltage probes is expected to be considerably smaller than the number of interparticle contacts in typical powder-pellet resistance measurements[2]. The most important factor is the entanglement of ropes which results in a very low apparent density; and actual area transverse to the current direction is much smaller than the physical cross-section, typically by a factor of 50. We compensate approximately for this porosity by calculating ρ using an effective microscopic area determined from the mass and total length of the mat sample and an assumed microscopic density of $2\,g\,cm^{-3}$ (between that of graphite and solid C_{60}). For example, a typical mat sample, ~0.2 mm thick if measured with a calliper using light pressure, should weigh ~10 mg if the density was $2\,g\,cm^{-3}$, whereas the measured mass is only 200 μg.

We measured resistance as a function of time of exposure to Br_2 vapour, using an apparatus similar to that employed for the first doping experiments on solid C_{60} (ref. 12). A few drops of Br_2 were initially frozen with liquid nitrogen in the bottom half of a 1-inch-diameter glass vessel equipped with an O-ring seal; the sample and lead frame were suspended from the upper half by the leads and glass-to-metal seals. Figure 1 shows that once the Br_2 was allowed to melt, the resistivity dropped from its initial value, 0.016 Ω cm, to 0.001 Ω cm in less than 4 minutes. Refreezing the Br_2 had little effect, as did opening the vessel and exposing the doped sample to air. Only by heating the sample with a heat gun for 5 minutes did ρ begin to recover. After cooling back to a temperature T of 300 K we found a stable plateau at 0.008 Ω cm, half the initial value. Re-doping with Br_2 again decreased ρ to 0.001 Ω cm , and these same limiting values were obtained on repeated cycling. In a separate experiment with a larger sample, we ascertained from weight uptake and loss the average compositions noted in Fig. 1.

We measured $\rho(T)$ on another sample before and after Br_2 doping and undoping, using a wide-temperature-range Joule–Thompson cryostat (Model R2205-23, MMR Technologies, Mountain View, California). Curve a in Fig. 2 shows the behaviour typical of pristine SWNT mats[2], namely a weakly metallic $\rho(T)$ above a crossover temperature T^* which for this sample is ~280 K. We have previously presented evidence that T^* correlates directly with disorder; snag-free single ropes have $T^* \approx 40$ K whereas material with a lower yield of SWNTs has T^* so high that positive $d\rho/dT$ is never observed. Curve b in Fig. 2 is for saturation doping, after transfer in air from the doping apparatus to the cryostat. In addition to the overall reduction in ρ, positive $d\rho/dT$ persists down to a much lower temperature than in the pristine material, below the limit (90 K) of the apparatus. Heating the sample to 450 K in the cryostat vacuum leads to an increase in ρ, curve c, while maintaining positive $d\rho/dT$.

The results in Figs 1 and 2 suggest the existence of (at least) two different Br populations, weakly and strongly bound, in the doped material. This is again reminiscent of intercalated graphite, in which even after long pumping and heating, some fraction of the intercalate is retained at defect sites in the so-called "residue compound"[5]. A second possibility is the existence of a stable phase with intermediate Br concentration, analogous to the staging phenomenon in graphite compounds.

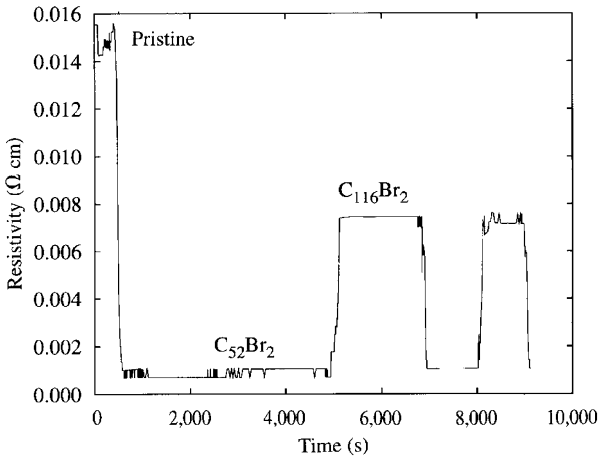

Figure 1 Directionally averaged resistivity (~300 K) of a bulk SWNT sample versus time of exposure to Br_2 vapour. Within 3 min, ρ has dropped from 0.015 to 0.001 Ω cm, with weight uptake (determined in a separate experiment) corresponding approximately to $C_{52}B_2$. After 3,000 s, the apparatus was opened to the air, with no change in ρ. After 5,000 s, the sample was heated in air with a heat gun for ~200 s, which increased ρ to 0.008 Ω cm and decreased the Br_2 content as shown. Re-exposing the same sample to Br_2 vapour at 7,000 s returned ρ to its previous minimum value. One additional heating/re-doping cycle is included in the figure.

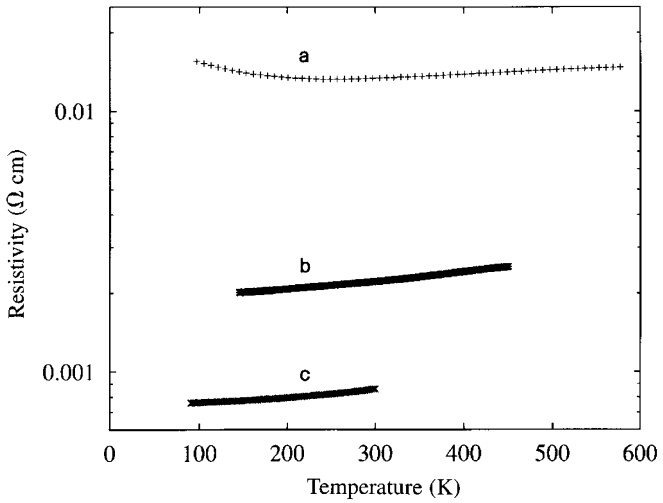

Figure 2 Resistivity versus temperature for a bulk SWNT sample. Curve a, pristine material; curve b, saturation doped with Br_2; curve c, after heating in the cryostat vacuum to 450 K for several hours.

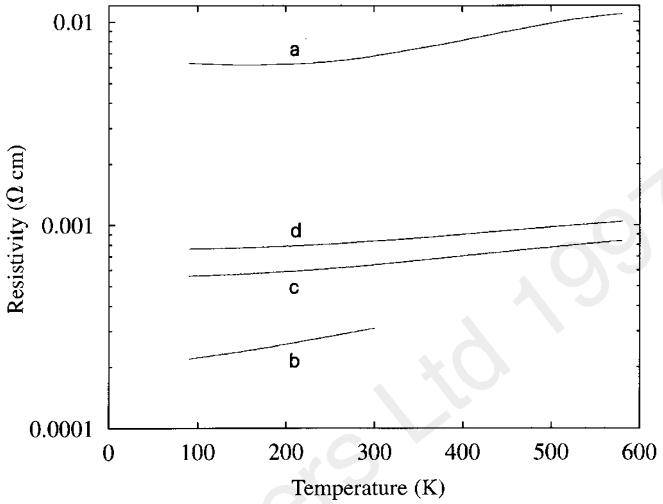

Figure 3 Resistivity versus temperature for a bulk SWNT sample. Curve a, pristine material (different batch than in Fig. 2); curve b, after doping with potassium at 473 K; curve c, after heating in the cryostat vacuum to 580 K overnight; curve d, after 3 d at 580 K.

Potassium doping also leads to a large enhancement in conductivity. Potassium metal was distilled into a glass tube containing a mat sample, sealed off, and reacted (473 K for 1–2 days) with a small temperature gradient to avoid coating the mat with K metal. Weight uptakes under these conditions correspond approximately to KC_8. Figure 3 shows a series of $\rho(T)$ measurements on one such sample. Curve a for this pristine sample reveals a lower ρ and T^* than the initial curve in Fig. 1. Curve b was measured after transferring the doped sample in a glove box from the reaction tube into the cryostat. The overall reduction in ρ is a factor of ~20 at 300 K, and again T^* is reduced to below our 90 K measurement limit, curve b. Heating overnight to 580 K in the cryostat vacuum yielded curve c, from which we find a smaller $d\rho/dT$ slope with ρ still one-tenth of the pristine value. Finally, curve d resulted from 580 K vacuum anneal for 3 days, with only a small additional resistivity increase. Similar to the Br_2 experiments above and in agreement with Raman data[13], we find considerable high-temperature stability of the reduction in resistivity. This suggests either strong bonding of part of the dopant at defect sites or the existence of stable intermediate phases; the former is characteristic of graphite compounds[5] whereas examples of the latter occur in alkali-doped fullerides[6]. In contrast to Br_2 doping, exposing this sample to air immediately led to a large increase in resistivity to several times greater than the pristine values.

The above results are consistent with Raman scattering data for the same dopants presented in the accompanying report[13], indicating that for K or Br_2, substantial electron density is respectively added or removed from the host carbon framework. The natural interpretation is that either electron or hole doping accompanies reductive or oxidative intercalation, as in graphite, with enhanced metallic behaviour in either case owing to increased carrier density. It is highly unlikely that the enhanced metallic behaviour results from reactions of K or Br_2 with minor constituents of our SWNT samples—principally amorphous carbon and residual Ni/Co catalyst particles encapsulated by graphitic 'onions'. Electron microscopy shows that both are widely dispersed and thus unlikely to form a macroscopic conducting path. In separate experiments we determined that Br_2 vapour has only a minor effect on the "amorphous" carbons typically studied for lithium-ion battery applications[14]. Furthermore the graphite skin on the Ni/Co particles must be free of defects and discontinuities as it resists attempts to remove the metal by intercalation followed by acid leaching—material thus treated remains magnetic.

Doping with K or Br_2 also yields important changes in the overall $\rho(T)$ behaviour. The net effect is a reduction in the crossover temperature T^*, above which the sign of $d\rho/dT$ changes from negative to positive. Balents and Fisher[15] conjectured that the crossover in pristine material can be understood as two additive contributions; for example, with T exponents of opposite sign[2]. From Figs 2 and 3, we see that the primary doping effect on $\rho(T)$ is a 'rigid' reduction with little or no change in slope, which would cause T^* to increase if the low-T component were unaffected. Furthermore, if $\rho(T)$ in the high-T regime were limited by electron–electron interactions[15], one would expect a doping-induced slope change, or at least important differences between K- and Br_2-doping. Although there appears to be a direct correlation between T^* and disorder[2], it is hard to imagine that the pristine material is more disordered than the doped material. Measurements below 90 K to probe the effects of doping on the negative slope contribution will be important to understand this effect. X-ray experiments to locate the K and Br dopants are in progress. Also of interest is the possibility of 'tuning' the electron transfer so that the Fermi energy coincides with a one-dimensional singularity in the electronic density of states[16], in which case one might be able to overcome the intrinsically weak electron–phonon interaction with a large density of states at the Fermi level to obtain superconductivity. A novel approach, unique to single-walled tubes, would be to exploit the quantum phenomena observed at very low temperatures[3,4]; doping-induced shifts in conductance peaks versus voltage should be directly related to the displacement in Fermi energy. □

Received 21 February; accepted 12 May 1997.

1. Thess, A. *et al.* Crystalline ropes of metallic carbon nanotubes. *Science* **273,** 483–487 (1996).
2. Fischer, J. E. *et al.* Metallic resistivity in crystalline ropes of single-wall carbon nanotubes. *Phys. Rev. B* **55,** R4921–R4924 (1997).
3. Tans, S. J. *et al.* Individual single-wall nanotubes as quantum wires. *Nature* **386,** 474–476 (1997).
4. Bockrath, M. *et al.* Single-electron transport in ropes of carbon nanotubes. *Science* **275,** 1922–1925 (1997).
5. Zabel, H. & Solin, S. A. (eds) *Graphite Intercalation Compounds II: Transport and Electronic Properties* (Springer, New York, 1992).
6. Rosseinsky, M. J. Fullerene intercalation chemistry. *J. Mater. Chem.* **5,** 1497–1513 (1995).
7. Zhou, O. *et al.* Defects in carbon nanostructures. *Science* **263,** 1744–1747 (1994).
8. Mordkovich, V. Z., Baxendale, M., Yoshimura, S. & Chang, R. P. H. Intercalation into carbon nanotubes. *Carbon* **34,** 1301–1303 (1996).
9. Cowley, J. M., Nikolaev, P., Thess, A. & Smalley, R. E. Electron nano-diffraction study of carbon single-walled nanotube ropes. *Chem. Phys. Lett.* **265,** 379–384 (1997).

10. Rao, A. M. *et al.* Diameter-selective Raman scattering from vibrational modes in carbon nanotubes. *Science* **275,** 187–191 (1997).
11. Kane, C. L. & Mele, E. J. Size, shape, and low-energy electronic structure of carbon nanotubes. *Phys. Rev. Lett.* **78,** 1932–1935 (1997).
12. Haddon, R. C. *et al.* Conducting films of C_{60} and C_{70} by alkali metal doping. *Nature* **350,** 320–232 (1991).
13. Rao, A. M., Eklund, P. C., Bandow, S., Thess, A. & Smalley, R. E. Evidence for charge transfer in doped carbon nanotube bundles from Raman scattering. *Nature* **388,** 257–259 (1997).
14. Dahn, J. R., Zheng, T., Liu, Y. H. & Xue, J. S. Mechanisms for lithium insertion in carbonaceous materials. *Science* **270,** 590–593 (1995).
15. Balents, L. & Fisher, M. P. A. Correlation effects in carbon nanotubes. *Phys. Rev. Lett.* **55,** 11973–11976 (1997).
16. Mintmire, J. W., Robertson, D. H. & White, C. T. Properties of fullerene nanotubes. *J. Phys. Chem. Solids* **54,** 1835–1840 (1993).

Acknowledgements. H.J.K. is on leave from Hallym University, South Korea. We thank M. Clement for experimental assistance. Work at Penn was supported by the Department of Energy; work at Rice was supported by the Office of Naval Research and the Robert A. Welch Foundation.

Correspondence and requests for materials should be addressed to J.E.F. (e-mail: fischer@sol1.lrsm.upenn.edu).

Evidence for charge transfer in doped carbon nanotube bundles from Raman scattering

A. M. Rao*, P. C. Eklund*, Shunji Bandow†, A. Thess‡ & R. E. Smalley‡

* *Department of Physics and Astronomy and Center for Applied Energy Research, University of Kentucky, Lexington, Kentucky 40506–0055, USA*
† *Instrument Center, Institute for Molecular Science, Myodaiji, Okazaki, 444, Japan*
‡ *Center for Nanoscale Science and Technology, Rice Quantum Institute and Departments of Chemistry and Physics, Rice University, Houston, Texas 77251, USA*

Single-walled carbon nanotubes[1] (SWNTs) are predicted to be metallic for certain diameters and pitches of the twisted graphene ribbons that make up their walls[2]. Chemical doping is expected to substantially increase the density of free charge carriers and thereby enhance the electrical (and thermal) conductivity. Here we use Raman spectroscopy to study the effects of exposing SWNT bundles[1] to typical electron-donor (potassium, rubidium) and electron-acceptor (iodine, bromine) dopants. We find that the high-frequency tangential vibrational modes of the carbon atoms in the SWNTs shift substantially to lower (for K, Rb) or higher (for Br_2) frequencies. Little change is seen for I_2 doping. These shifts provide evidence for charge transfer between the dopants and the nanotubes, indicating an ionic character of the doped samples. This, together with conductivity measurements[3], suggests that doping does increase the carrier concentration of the SWNT bundles.

We generate SWNT bundles by a dual pulsed-laser technique[1], which is known to produce a very narrow diameter distribution peaked around the diameter of the (10,10) ('armchair') nanotube (here the indices refer to the diameter and pitch of the tubes). The nanotubes are grouped into aligned bundles of as many as 100–500 tubes, packed into a triangular lattice. The chemical doping of the SWNT bundles was carried out in sealed quartz ampoules using vapour-distilled reactants. Our method parallels those used to intercalate graphite[4]. In the SWNT bundles studied here, the dopant is not expected to lie inside the tube; it may be confined to the interstitial channels found between the tubes in the bundles, or may decorate the entire exterior surface of the SWNTs. If the tubule ends were open, however, it should also be possible to place dopant ions or molecules inside the tubes, as has been done with very small (~1.2 nm inside diameter) multi-wall nanotubes[5,6].

The reactant and SWNT sample were positioned at opposite ends of an evacuated ampoule; the reactant vapour travels to the far end of the ampoule where the reaction takes place. The reaction with I_2 and Br_2 were carried out with both the sample and reactant at room temperature; the reaction is quite fast with Br_2 (minutes), whereas I_2 requires several hours to saturate the sample. The alkali-metal reactions were both carried out with the alkali metal and SWNTs at elevated temperatures for 24 h (metal temperature, 120 °C; SWNT temperature, 160 °C). Raman scattering spectra were then measured while the samples remained sealed in their reaction ampoules. All the spectra reported here were measured in the backscattering configuration using 514.5-nm laser excitation. The scattered light was analysed in a Jobin Yvon HR460 single-grating spectrometer equipped with a charge-coupled array detector and a holographic notch filter (Kaiser Optical Systems, Inc., Ann Arbor, MI, USA). To avoid laser damage to the sample, all the data were taken at low laser power (2 W cm^{-2}) using a cylindrical lens to focus the laser radiation onto the sample (which was a loosely compacted mat of SWNTs). No polarization analyser was used, so that light polarized both perpendicular and parallel to the scattering plane was collected. Figure 1 shows the $T = 300$ K Raman spectra of pristine SWNTs and those doped with the anticipated electron-acceptor (I_2, Br_2) and electron-donor (K, Rb) reagents.

We first discuss briefly the Raman spectrum for pristine SWNTs (Fig. 1, middle spectrum). As discussed previously[7], the strong peak at 186 cm^{-1} has been identified with the A_g symmetry radial breathing mode, and the peak at 1,593 cm^{-1} has been assigned to an unresolved Raman triplet identified with tangential C-atom displacement modes, one of A_g and two with E_g symmetry. These three, nearly degenerate, tubule phonons are related to phonons in the highest-frequency optical phonon branch of graphite which exhibits a zone centre E_{2g} symmetry intralayer mode at 1,582 cm^{-1}. The relative peak intensities of all the Raman-active modes depend critically on the laser wavelength which indicates that the scattering is resonant[7]. For the assignments of the weaker peaks in the pristine spectrum, see ref. 7.

We next address the changes in the Raman spectrum of the pristine tubes due to chemical doping (Fig. 1). The top two spectra in Fig. 1 are for SWNT bundles reacted with typical electron-acceptor dopants (I_2, Br_2) which are expected to transfer electrons from the carbon π states in the tubules to the dopant molecules, creating hole carriers in the SWNTs. The I_2-doping induces the smallest change in the SWNT Raman spectrum. This is perhaps not surprising, as I_2 does not intercalate into graphite. It does diffuse into solid C_{60} (refs 8, 9), but no convincing evidence for charge transfer with the fullerene lattice has been reported. For the chemically doped SWNTs, we assign the most intense low-frequency and high-frequency modes to the radial and tangential modes, respectively. Iodine-doping of SWNT bundles is seen to slightly increase the radial mode frequency from 186 to 188 cm^{-1} ($\Delta_r = +2\ cm^{-1}$), and slightly decrease the tangential mode frequencies from 1,593 cm^{-1} in the pristine SWNT to 1,590 cm^{-1} ($\Delta_t = -3\ cm^{-1}$), where Δ_r and Δ_t refer to the change in the radial and tangential mode frequencies on doping. For the case of saturated Br_2-doping, relatively large increases in the radial and tangential mode frequencies are observed: $\Delta_r = +74\ cm^{-1}$ and $\Delta_t = +24\ cm^{-1}$. We note that the 1,617 cm^{-1} peak in the Br_2-doped SWNT decreases in frequency to 1,603 cm^{-1} on refreezing the bromine vapour at the opposite end of the reaction tube; that is, the peak does not shift all the way back to the pristine value at 1,593 cm^{-1}. This suggests the existence of an intermediate-concentration Br_2-doped phase, in agreement with the resistivity studies on Br_2-doped SWNT[3]. Also in agreement with these resistivity studies[3], the Raman spectrum of saturated Br_2-doped SWNT bundles shown in Fig. 1 is recovered again when the Br_2 returns to room temperature and the increased vapour pressure drives the Br_2–SWNT system back to the Br_2-saturated phase.